Commensurate mixtures of ultra-cold atoms in one dimension

L. Mathey

Physics Department, Harvard University, Cambridge, MA 02138

(Dated: February 6, 2008)

We study binary mixtures of ultra-cold atoms, confined to one dimension in an optical lattice, with commensurate densities. Within a Luttinger liquid description, which treats various mixtures on equal footing, we derive a system of renormalization group equations at second order, from which we determine the rich phase diagrams of these mixtures. These phases include charge/spin density wave order, singlet and triplet pairing, polaron pairing[9], and a supersolid phase. Various methods to detect our results experimentally are discussed.

I. INTRODUCTION

Recent advances in controlling ultra cold atoms lead to the realization of truly one dimensional systems, and the study of many-body effects therein. Important benchmarks, such as the Tonks-Girardeau gas[1,2] and the Mott transition in one dimension[3], have been achieved by trapping bosonic atoms in tight tubes formed by an optical lattice potential. Novel transport properties of one dimensional lattice bosons have been studied using these techniques[4]. More recently, a strongly interacting one dimensional Fermi gas was realized using similar trapping methods[5]. Interactions between the fermion atoms were controlled by tuning a Feshbach resonance in these experiments. On the theory side, numerous proposals were given for realizing a variety of different phases in ultra cold Fermi systems[6,7], Bose-Fermi mixtures[8,9,10,11], as well as Bose-Bose mixtures[12]. In [13], commensurate mixtures in higher dimensions were studied.

In this paper we explore the behavior of ultracold atomic mixtures, confined to one-dimensional (1D) motion in an optical lattice, that exhibit different types of commensurability, by which we mean that the atomic densities and/or the inverse lattice spacing have an integer ratio. Commensurable fillings arise naturally in many ultracold atom systems, because the external trap potential approximately corresponds to a sweep of the chemical potential through the phase diagram, and therefore passes through points of commensurability. At these points the system can develop an energy gap, which fixes the density commensurability over a spatially extended volume. This was demonstrated in the celebrated Mott insulator experiment by Greiner et al.[14], where Mott phases with integer filling occurred in shell-shaped regions in the atom trap. These gapped phases gave rise to the well-known signature in the time-of-flight images[15], and triggered the endeavor of 'engineering' many-body states in optical lattices. Further examples include the recently created density-imbalanced fermion mixtures[16] in which the development of a balanced, i.e. commensurate, mixture at the center of the trap is observed.

In 1D, this phenomenon is of particular importance, because it is the only effect that can lead to the opening of a gap, for a system with short-range interactions.

In contrast to higher dimensional systems, where, for instance, pairing can lead to a state with an energy gap, in 1D only discrete symmetries can be broken, due to the importance of fluctuations. Orders that correspond to a continuous symmetry can, at most, develop quasi long range order (QLRO), which refers to a state in which an order parameter $O(x)$ has a correlation function with algebraic scaling, $\langle O(x)O(0)\rangle \sim |x|^{-(2-\alpha)}$, with a positive scaling exponent α.

Due to its importance in solid state physics, the most thoroughly studied commensurate 1D system is the SU(2) symmetric system of spin-1/2 fermions. This system develops a spin gap for attractive interaction and remains gapless for repulsive interaction, as can be seen from a second order RG calculation. However, the assumed symmetry between the two internal spin states, which is natural in solid state systems, does not generically occur in Fermi-Fermi mixtures (FFMs) of ultra-cold atoms, where the 'spin' states are in fact different hyperfine states of the atoms. An analysis of the generic system is therefore highly called for. Furthermore, we will extend this analysis to both Bose-Fermi (BFMs) and Bose-Bose mixtures (BBMs), as well as to the dual commensurability, in which the charge field, and not the spin field, exhibits commensurate filling, as will be explained below.

The main results of this paper are the phase diagrams shown in Fig. 1–4. We find that both attractive and repulsive interactions can open an energy gap. For FFMs the entire phase diagram is gapped, except for the repulsive SU(2) symmetric regime (cp. [7]), for BFMs or BBMs the bosonic liquid(s) need(s) to be close to the hardcore limit, otherwise the system remains gapless. Furthermore, we find a rich structure of quasi-phases, including charge and spin density wave order (CDW, SDW), singlet and triplet pairing (SS, TS), polaron pairing[9,10], and a supersolid phase, which is the first example of a supersolid phase in 1D. These results are derived within a Luttinger liquid (LL) description, which treats bosonic and fermionic liquids on equal footing.

This paper is organized as follows: In Section II we classify the different types of commensurate mixtures that can occur, and in Section III we discuss the effective action of the mixtures with the most relevant com-

mensurability term. In Section IV we discuss the set of renormalization group equations for such systems, and in Section V, VI, and VII, we apply these results to Fermi-Fermi, Bose-Bose, and Bose-Fermi mixtures, respectively. In Section VIII, we discuss the experimental detectibility, and in Section IX we conclude.

II. CLASSIFICATION OF COMMENSURATE MIXTURES

We will now classify the types of commensurability that can occur in a system with short-ranged density-density interaction. We consider Haldane's representation[18] of the densities for the two species:

$$n_{1/2} = [\nu_{1/2} + \Pi_{1/2}] \sum_m e^{2mi\Theta_{1/2}} \quad (1)$$

ν_1 and ν_2 are the densities of the two liquids, $\Pi_{1/2}(x)$ are the low-k parts (i.e. $k \ll 1/\nu$) of the density fluctuations; the fields $\Theta_{1/2}(x)$ are given by $\Theta_{1/2}(x) = \pi\nu_{1/2}x + \theta_{1/2}(x)$, with $\theta_{1/2}(x) = \pi \int^x dy \Pi_{1/2}(y)$. These expressions hold for both bosons and fermions. If we use this representation in a density-density interaction term $U_{12} \int dx n_1(x) n_2(x)$, we generate to lowest order a term of the shape $U_{12} \int dx \Pi_1(x) \Pi_2(x)$, but in addition an infinite number of nonlinear terms, corresponding to all harmonics in the representation. However, only the terms for which the linear terms $(2\pi m_{1/2}\nu_{1/2}x)$ cancel, can drive a phase transition. For a continuous system this happens for $m_1\nu_1 - m_2\nu_2 = 0$, whereas for a system on a lattice we have the condition $m_1\nu_1 - m_2\nu_2 = m_3$, where m_1, m_2 and m_3 are integer numbers. In general, higher integer numbers correspond to terms that are less relevant, because the scaling dimension of the non-linear term scales quadratically with these integers. We are therefore lead to consider small integer ratios between the fillings and/or the lattice if present. In [10], we considered two cases of commensurabilities: a Mott insulator transition coupled to an incommensurate liquid, and a fermionic liquid at half-filling coupled to an incommensurate bosonic liquid. In both cases the commensurability occurs between one species and the lattice, but does not involve the second species. In this paper we consider the two most relevant, i.e. lowest order, cases which exhibit a commensurability that involves both species. The first case is the case of equal filling $\nu_1 = \nu_2$, the second is the case of the total density being unity, i.e. $\nu_1 + \nu_2 = 1$, where the densities ν_1 and ν_2 themselves are incommensurate. The first case can drive the system to a spin-gapped state, the second to a charge gapped state. We will determine in which parameter regime these transitions occur, and what type of QRLO the system exhibits in the vicinity of the transition. These two cases can be mapped onto each other via a dual mapping, which enables us to study only one case and then infer the results for the second by using this mapping. We will write
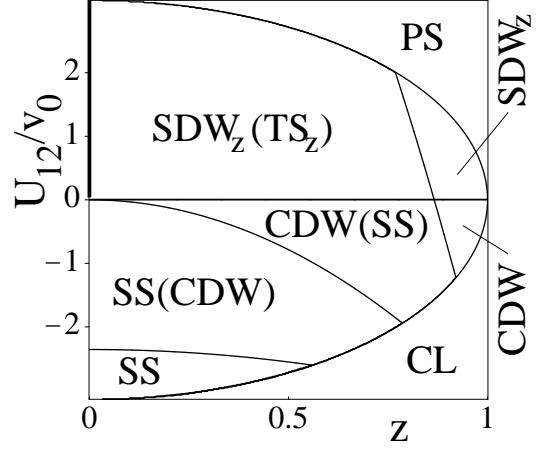

FIG. 1: Phase diagram of a commensurate FFM or a BBM of hardcore bosons (with the replacement $TS_z \to SS$), in terms of the interaction U_{12} and the parameter $z = |v_1 - v_2|/(v_1 + v_2)$. For both attractive and repulsive interactions a spin gap opens, except for $z = 0$ and positive interaction. In the attractive regime, a FFM or a BBM shows either singlet pairing or CDW order, or a coexistence of these phases. For repulsive interaction these mixtures show SDW ordering, with FFMs and BBMs showing subdominant triplet or singlet pairing, respectively, for a large range of z. In the gapless regime, a FFM shows degenerate SDW and CDW order, and a BBM shows SF with subdominant CDW, i.e. supersolid behavior. For very large positive values of U_{12} the system undergoes phase separation (PS); for very large negative values it collapses (CL).

out our discussion for the case of equal filling and merely state the corresponding results for complementary filling.

III. EFFECTIVE ACTION

The action of a two-species mixture with equal filling in bosonized form is given by:

$$S = S_{0,1} + S_{0,2} + S_{12} + S_{int}. \quad (2)$$

The terms $S_{0,j}$, with $j = 1, 2$, are given by

$$S_{0,j} = \frac{1}{2\pi K_j} \int d^2r \Big(\frac{1}{v_j}(\partial_\tau \theta_j)^2 + v_j(\partial_x \theta_j)^2 \Big) \quad (3)$$

Each of the two types of atoms, regardless of being bosonic or fermionic, are characterized by a Luttinger parameter $K_{1/2}$ and a velocity $v_{1/2}$. Here we integrate over $\mathbf{r} = (v_0\tau, x)$, where we defined the energy scale $v_0 = (v_1 + v_2)/2$. The term S_{12} describes the acoustic coupling between the two species, and is bilinear:

$$S_{12} = \frac{U_{12}}{\pi^2} \int d^2r \partial_x \theta_1 \partial_x \theta_2 + \frac{V_{12}}{\pi^2} \int d^2r \partial_\tau \theta_1 \partial_\tau \theta_2. (4)$$

The second term is created during the RG flow; its prefactor therefore has the initial value $V_{12}(0) = 0$. We define

$S_0 = S_{0,1} + S_{0,2} + S_{12}$, which is the diagonalizable part of the action. S_{int} corresponds to the non-linear coupling between the two liquids, which we study within an RG approach:

$$S_{int} = \frac{2g_{12}}{(2\pi\alpha)^2} \int d^2r \cos(2\theta_1 - 2\theta_2). \qquad (5)$$

This bosonized description applies to a BBM, a BFM, and a FFM. Depending on which of these mixtures we want to describe we either construct bosonic or fermionic operators according to Haldane's contruction[18]:

$$f/b = [\nu_0 + \Pi]^{1/2} \sum_{m\,odd/even} e^{mi\Theta}e^{i\Phi}. \qquad (6)$$

ν_0 is the zero-mode of the density, $\Phi(x)$ is the phase field, which is the conjugate field of the density fluctuations $\Pi(x)$. The action for a mixture with complementary filling, $\nu_1 + \nu_2 = 1$, is of the form $S_0 + S'_{int}$, where the interaction S'_{int} is given by:

$$S'_{int} = \frac{2g_{12}}{(2\pi\alpha)^2} \int d^2r \cos(2\theta_1 + 2\theta_2). \qquad (7)$$

To map the action in Eq. (2) onto this system we use the mapping: $\theta_2 \rightarrow -\theta_2$, $\phi_2 \rightarrow -\phi_2$, and $g_{12} \rightarrow -g_{12}$, which evidently maps a mixture with complementary filling and attractive (repulsive) interaction and onto a mixture with equal filling with repulsive (attractive) interaction.

IV. RENORMALIZATION GROUP

To study the action given in Eq. (2), we perform an RG calculation along the lines of the treatment of the sine-Gordon model in [21]. In our model, a crucial modification arises: the linear combination $\theta_1 - \theta_2$, that appears in the non-linear term, is not proportional to an eigenmode of S_0, and therefore the RG flow does not affect only one separate sector of the system, as in an SU(2)-symmetric system. The RG scheme that we use here proceeds as follows: First, we diagonalize S_0 through the transformation

$$\theta_1 = B_1\tilde{\theta}_1 + B_2\tilde{\theta}_2, \qquad (8)$$
$$\theta_2 = D_1\tilde{\theta}_1 + D_2\tilde{\theta}_2. \qquad (9)$$

The coefficients $B_{1/2}$ and $D_{1/2}$ are given in the Appendix. The fields $\tilde{\theta}_{1/2}$ are the eigenmode fields with velocities $\tilde{v}_{1/2}$ (see Appendix). As the next step, we introduce an energy cut-off Λ on the fields $\tilde{\theta}_{1/2}$ according to $\omega^2/\tilde{v}_{1/2} + \tilde{v}_{1/2}k^2 < \Lambda^2$. We shift this cut-off by an amount $d\Lambda$, and correct for this shift up to second order in g_{12}. At first order, only g_{12} is affected, its flow equation is given by:

$$\frac{dg_{12}}{dl} = \left(2 - K_1 - K_2 - \frac{2}{\pi}\frac{U_{12} + V_{12}v_1v_2}{v_1 + v_2}\right)g_{12}, (10)$$
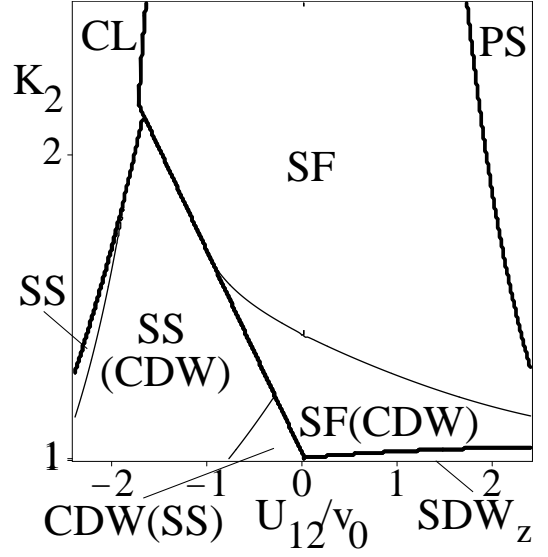

FIG. 2: Phase diagram of a BBM with the first species being in the hardcore limit, in terms of U_{12}, and the Luttinger parameter of the second species (K_2), at the fixed velocity ratio $|v_1 - v_2|/(v_1 + v_2) = 0.5$. For large repulsive interaction the system undergoes phase separation (PS), for large attractive interaction the system collapses (CL). In the regime below the thick line the system opens a gap, i.e. if species 2 is close to the hardcore limit. However, for larger values of K_2, the gapless phase is restored. Close to the transition, the properties of the hardcore bosons, are affected by the RG flow, leading to supersolid behavior.

with $dl = d\Lambda/\Lambda$. At second order several terms are created that are quadratic in the original fields θ_1 and θ_2. We undo the diagonalization, Eq. (8) and (9), and absorb these terms into the parameters of the action, which concludes the RG step. By iterating this procedure we obtain these flow equations at second order in g_{12}:

$$\frac{dK_{1/2}}{dl} = -\frac{g_{12}^2}{16\pi^2}\left(2 + \left(\frac{v_2}{v_1} + \frac{v_1}{v_2}\right)\right) \qquad (11)$$

$$\frac{dv_1}{dl} = v_1\frac{g_{12}^2}{16\pi^2}\left(\frac{v_2}{v_1} - \frac{v_1}{v_2}\right) \qquad (12)$$

$$\frac{dv_2}{dl} = v_2\frac{g_{12}^2}{16\pi^2}\left(\frac{v_1}{v_2} - \frac{v_2}{v_1}\right) \qquad (13)$$

$$\frac{dU_{12}}{dl} = -\frac{g_{12}^2}{8\pi}(v_1 + v_2) \qquad (14)$$

$$\frac{dV_{12}}{dl} = -\frac{g_{12}^2}{8\pi}(1/v_1 + 1/v_2) \qquad (15)$$

A similar set of equations has been derived in [7] for a FFM in non-bosonized form. The difference between our result and the result in [7] is the renormalization of the velocities, that we find here, which is due to different types of expansions: In [7] only one-loop contributions are taken into account, whereas here we use a cumulant expansion in g_{12}, which at second order includes contributions that are two-loop for the renormalization of the velocities. These contributions, which would integrate to

zero for equal velocities, as can be seen from Eqns. 12 and 13, leads to the discrepancy between the expansion in the number of loops and the cumulant expansion, and gives a small quantitative correction of the velocities. As mentioned before, the advantage of the current approach is that the QRLO of the system can be directly determined from the resulting renormalized parameters, and that the same action can be used to study BBMs and BFMs.

The system of differential equations, Eqns. (10) to (15), can show two types of qualitative behavior: The coefficient g_{12} of the non-linear term (5) can either flow to zero, i.e. S_{int} is irrelevant, or it diverges, leading to the formation of an energy gap. In the first case, the system flows to a fixed point that is described by a renormalized diagonalizable action of the type S_0, from which the quasi-phases can be determined.

When S_{int} is relevant, we introduce the fields[19] $\theta_{\rho/\sigma} = \frac{1}{\sqrt{2}}(\theta_1 \pm \theta_2)$, which define the charge and the spin sector of the system. In this regime, these sectors decouple. Each of the two sectors is characterized by a Luttinger parameter and a velocity, $K_{\rho/\sigma}$ and $v_{\rho/\sigma}$, which are related to the original parameters in S_0 in a straightforward way. Using the numerical solution of the flow equations, we find that $K_\sigma \to 0$, as can be expected for an ordering of the nature of a spin gap, leaving K_ρ the only parameter characterizing the QLRO in this phase.

In order to determine the QLRO in the system we determine the scaling exponents of various order parameters. For that purpose, we use the bosonization representation of these order parameters, which contain the fields $\theta_{1/2}$ and $\phi_{1/2}$, and use the diagonalization, Eqs. (8) and (9), for the fields $\theta_{1/2}$, as well as the dual transformation for the fields $\phi_{1/2}$:

$$\phi_1 = C_1 \tilde{\phi}_1 + C_2 \tilde{\phi}_2, \tag{16}$$
$$\phi_2 = E_1 \tilde{\phi}_1 + E_2 \tilde{\phi}_2. \tag{17}$$

The coefficients $C_{1/2}$ and $D_{1/2}$ are given in the Appendix. Since the order parameters are now written in terms of the eigenfields $\tilde{\theta}_{1/2}$ and $\tilde{\phi}_{1/2}$, the correlation functions can be evaluated in a straight forward manner. The scaling exponents are given by various quadratic expressions of the parameters in Eqs. (8), (9), (16), and (17). In [10], we give an extensive list of correlation functions, which can be transferred to the system considered here, with the formal replacement: $\beta_{1/2} \to B_{1/2}$, $\gamma_{1/2} \to C_{1/2}$, $\delta_{1/2} \to D_{1/2}$, and $\epsilon_{1/2} \to E_{1/2}$. The order parameter with the largest positive scaling exponent shows the dominant order, whereas other orders with positive exponent are subdominant.

V. FERMI-FERMI MIXTURES

We will now apply this procedure to the different types of mixtures. For a FFM we find that the system always develops a gap, with the exception of the repulsive SU(2)
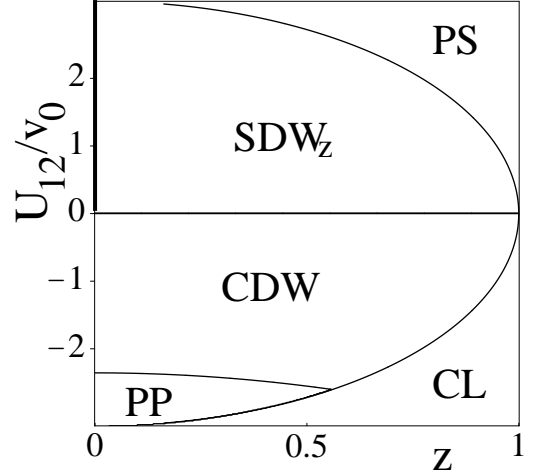

FIG. 3: Phase diagram of a BFM with hardcore bosons, in terms of the interaction U_{12} and the parameter $z = |v_1 - v_2|/(v_1 + v_2)$. For both attractive and repulsive interactions a spin gap opens, except for $z = 0$ and positive interaction. In the attractive regime, a BFM shows either CDW order or polaron pairing; for repulsive interaction BFMs show SDW ordering. In the gapless regime, a BFM shows CDW order for the fermions and SF for the bosons. For very large positive values of U_{12} the system undergoes phase separation (PS); for very large negative values it collapses (CL).

symmetric regime (cp. [7]). To determine the QLRO we introduce the following operators[19,20]:

$$O_{SS} = \sum_{\sigma,\sigma'} \tilde{\sigma} f_{R,\sigma} \delta_{\sigma,\sigma'} f_{L,3-\sigma'}, \tag{18}$$

$$O_{TS}^a = \sum_{\sigma,\sigma'} \tilde{\sigma} f_{R,\sigma} \sigma_{\sigma,\sigma'}^a f_{L,3-\sigma'}, \tag{19}$$

$$O_{CDW} = \sum_{\sigma,\sigma'} f_{R,\sigma}^\dagger \delta_{\sigma,\sigma'} f_{L,\sigma'}, \tag{20}$$

$$O_{SDW}^a = \sum_{\sigma,\sigma'} \tilde{\sigma} f_{R,\sigma}^\dagger \sigma_{\sigma,\sigma'}^a f_{L,\sigma'}, \tag{21}$$

with $\sigma, \sigma' = 1, 2$, $\tilde{\sigma} = 3 - 2\sigma$, and $a = x, y, z$. In the gapless SU(2) symmetric regime, both CDW and SDW show QLRO, with both scaling exponents of the form $\alpha_{SDW/CDW} = 1 - K_\rho$[19], which shows that these orders are algebraically degenerate. Within the gapped regime the scaling exponents of these operators are given by $\alpha_{SS,TS_z} = 2 - K_\rho^{-1}$ and $\alpha_{CDW,SDW_z} = 2 - K_\rho$. As discussed in [20], the sign of g_{12} determines whether CDW or SDW$_z$, and SS or TS$_z$ appears. In Fig. 1, we show the phase diagram based on these results. In addition to these phases we indicate the appearance of the Wentzel-Bardeen instability, shown as phase separation for repulsive interaction and collapse for attractive interaction.

We will now use the dual mapping to obtain the phase diagram of a FFM with complementary filling from Fig. 1. Under this mapping, the attractive and repulsive regimes are exchanged with the following replacements:

$CDW{\to}SDW_z$, $SDW_z{\to}CDW$, $SS,TS_z{\to}SDW$, and $SDW{\to}SS$. Note that the gapless regime is now on the attractive side, with degenerate CDW and SS pairing.

VI. BOSE-BOSE MIXTURES

For BBMs we proceed in the same way as for FFMs. We introduce the following set of order parameters:

$$O_{CDW} = b_1^\dagger b_1 + b_2^\dagger b_2, \tag{22}$$

$$O_{SS} = b_1 b_2, \tag{23}$$

$$O_{SDW_z} = b_1^\dagger b_1 - b_2^\dagger b_2, \tag{24}$$

$$O_{SDW_x} = b_1^\dagger b_2 + b_2^\dagger b_1, \tag{25}$$

$$O_{SDW_y} = -i(b_1^\dagger b_2 - b_2^\dagger b_1), \tag{26}$$

and in addition the superfluid (SF) order parameters b_1 and b_2. In Fig. 1 we show the phase diagram of a mixture of a BBM of hardcore bosons, which is almost identical to the one of a FFM. The phase diagram of the mixture with complementary filling, as obtained from the dual mapping, is also of the same form as its fermionic equivalent, with the exception of the gapless regime, in which BBMs show supersolid behavior (coexistence of SF and CDW order), and with the replacement $TS_z{\to}SS$.

In Fig. 2, we show the phase diagram of a mixture of hardcore bosons (species 1) and bosons in the intermediate to hardcore regime (species 2). If species 2 is sufficiently far away from the hardcore limit, the system remains gapless. However, in the vicinity of the transition the scaling exponents of the liquids are affected by the RG flow. As indicated, the effective scaling exponent of the hardcore bosons is renormalized to a value that is smaller than 1, and therefore we find both SF and CDW order, i.e. supersolid behavior. The phase diagram of the dual mixture is of the following form: the attractive and the repulsive regime are exchanged, and in the gapped phase we again have the mapping: $CDW{\to}SDW_z$, $SDW_z{\to}CDW$, $SS{\to}SDW_{x,y}$, and $SDW_{x,y}{\to}SS$. The gapless regime is unaffected.

The paired SF state discussed in [13] corresponds to the SS phase discussed here, whereas the dual $SDW_{x,y}$ phase that appears for complementary filling corresponds to the super-counter-fluid phase described therein. Note that here these orders compete with either CDW or SDW_z order, and only appear as QLRO, not LRO, as in higher dimensions. Both of these insights can only be gained by the using the LL description and RG that is used in this paper.

VII. BOSE-FERMI MIXTURES

For a BFM we find that the order parameters O_{CDW}, O_{SDW_z}, the polaron pairing operator

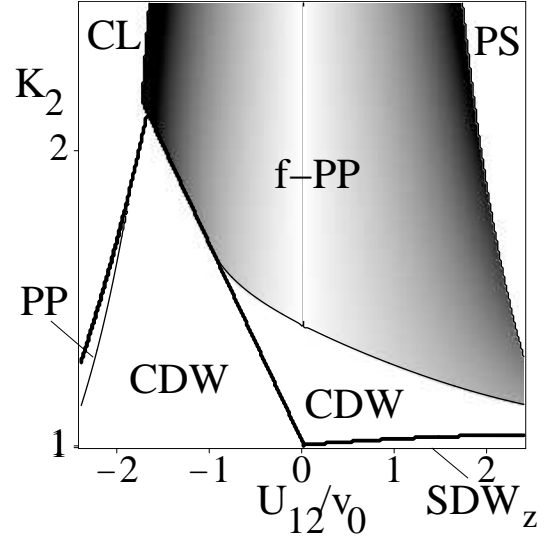$$O_{f-PP} = f_R f_L e^{-2i\lambda\Phi_b} \tag{27}$$

FIG. 4: Phase diagram of a BFM, in terms of U_{12}, and the Luttinger parameter of the second species (K_2), at the fixed velocity ratio $|v_1 - v_2|/(v_1 + v_2) = 0.5$. For large repulsive interaction the system undergoes phase separation (PS), for large attractive interaction the system collapses (CL). In the regime below the thick line the system opens a gap, i.e. if species 2 is close to the hardcore limit. However, for larger values of K_2, the gapless phase is restored. Close to the transition, the properties of the fermions, are still affected by the RG flow, leading to CDW order.

(see [9,10]), and b can develop QLRO in the gapless regime. In the gapped regime, the order parameters

$$O_{PP} \equiv f_R b f_L b, \tag{28}$$

$$O_{PP'} \equiv f_R b^\dagger f_L b^\dagger, \tag{29}$$

in addition to O_{CDW}, show QLRO. ($O_{PP/PP'}$ are special cases of the polaron pairing operator (27), extensively discussed in [9] and [10].) In Fig. 3 we show the phase diagram of a BFM with hardcore bosons, and in Fig. 4, we vary the Luttinger parameter of the bosons. In both the gapless phase and the gapped phase, we find that CDW and f-PP or PP, respectively, are mutually exclusive and cover the entire phase diagram, cp. [9,10]. The dual mapping again maps attractive and repulsive regimes onto each other. Within the gapped phase we find the mapping $CDW{\to}SDW_z$, $SDW_z{\to}CDW$, and $PP{\to}PP'$, the gapless regime is unaffected.

VIII. EXPERIMENTAL DETECTION

The phase diagrams that have been derived and shown in Figs. 1–4, are given in terms of the parameters that appear in the effective action. With such a field theoretical approach we can find the correct qualitative long-range behavior, such as the functional form of the correlation functions. However, it is also intrinsic to this approach

that the effective parameters appearing can only be qualitatively related to the underlying microscopic parameters. Based on a phase diagram such as Fig. 2, for instance, the following features for a mixture of bosonic atoms with a short-range interaction can be expected: If one species is in the hardcore limit, and the other is in between an intermediate interaction regime and the hardcore limit, then for attractive interaction between them, a gapped state can be created, in which there is a competition of SS pairing and CDW order. For repulsive interaction, and the second species being very close to the hardcore regime, one can also expect a gapped phase, in which we find SDW_z order. For the intermediate regime we expect a supersolid phase.

Before we conclude, we discuss how the predictions presented in this paper could be measured experimentally. Since the appearance of a gapped state has already been demonstrated for the MI-SF transition in 1D [3], and since it constitutes a significant qualitative change in the system, this would be the first feature predicted in this paper to look for. As demonstrated in [23], RF spectroscopy can be used to determine the presence and the size of an energy gap. To detect the rich structure of QLRO the following approaches can be taken: CDW order will create additional peaks in TOF images, corresponding to a wavevector $Q = 2k_f$. As demonstrated and pointed out in [22], the noise in TOF images allows to identify the different regimes of both gapped and gapless phases. As discussed in [9,10], a laser stirring experiment could determine the onset of CDW order for fermions, or the supersolid regime for bosons.

IX. CONCLUSION

In conclusion, we have studied mixtures of ultra-cold atoms in 1D with commensurate filling. We used a Luttinger liquid description which enables us to study FFMs, BFMs, and BBMs in a single approach. We find that FFMs are generically gapped for both attractive and repulsive interactions, whereas for BFMs and BBMs the bosons need to be close to the hardcore limit. We find a rich structure of quasi-phases in the vicinity of these transitions, in particular a supersolid phase for BBMs, that occurs close to the hardcore limit. Experimental methods to detect the predictions were also discussed.

APPENDIX A

Here we give the coefficients that appear in the transformations (8), (9), (16), and (17), that map the original fields on the eigenfields at each point in the RG flow. The coefficients $B_{1/2}$ and $D_{1/2}$ are given by:

$$B_1 = \beta_1\zeta_1 + \beta_2\kappa_1, \ B_2 = \beta_1\zeta_2 + \beta_2\kappa_2, \quad (A1)$$
$$D_1 = \delta_1\zeta_1 + \delta_2\kappa_1, \ D_2 = \delta_1\zeta_2 + \delta_2\kappa_2. \quad (A2)$$

The coefficients $\beta_{1/2}$ and $\delta_{1/2}$ are given in [9,10], where the indices 'f' and 'b' need to replaced by '1' and '2', respectively. The other coefficients are given by:

$$\zeta_1 = \sqrt{\tilde{v}_1/v_A}\cos\theta, \ \zeta_2 = \sqrt{\tilde{v}_2/v_A}\sin\theta, \quad (A3)$$
$$\kappa_1 = -\sqrt{\tilde{v}_1/v_a}\sin\theta, \ \kappa_2 = \sqrt{\tilde{v}_2/v_a}\cos\theta, \quad (A4)$$

where the angle θ is given by:

$$\tan 2\theta = -\tilde{V}_{12}/\sqrt{v_A v_a}(\tilde{v}_A^{-2} - \tilde{v}_a^{-2}), \quad (A5)$$

where we used:

$$\tilde{v}_A = v_A/\sqrt{1 + 2V_{12}v_A\beta_1\delta_1/\pi}, \quad (A6)$$
$$\tilde{v}_a = v_a/\sqrt{1 + 2V_{12}v_A\beta_2\delta_2/\pi}. \quad (A7)$$

The velocities $\tilde{v}_{1/2}$, corresponding to the eigenmodes $\tilde{\theta}_{1/2}$, are given by

$$\tilde{v}_{1/2}^{-2} = \frac{1}{2}(\tilde{v}_A^{-2} + \tilde{v}_a^{-2}) \pm \frac{1}{2}\sqrt{(\tilde{v}_A^{-2} - \tilde{v}_a^{-2})^2 + \tilde{V}_{12}^2 v_A^{-1} v_a^{-1}} \quad (A8)$$

where $\tilde{V}_{12}$ is given by

$$\tilde{V}_{12} = 2V_{12}(\beta_1\delta_2 + \beta_2\delta_1)/\pi. \quad (A9)$$

$v_{A,a}$ are defined as in [9,10]. The coefficients $C_{1/2}$ and $D_{1/2}$, that appear in the dual transformation, Eqs. (16) and (17), are given by:

$$C_1 = \gamma_1\eta_1 + \gamma_2\lambda_1, \ C_2 = \gamma_1\eta_2 + \gamma_2\lambda_2, \quad (A10)$$
$$E_1 = \epsilon_1\eta_1 + \epsilon_2\lambda_1, \ E_2 = \epsilon_1\eta_2 + \epsilon_2\lambda_2. \quad (A11)$$

$\gamma_{1/2}$ and $\epsilon_{1/2}$ are given in [9,10], with 'f' and 'b' replaced by '1' and '2', and $\eta_{1/2}$ and $\lambda_{1/2}$ given by:

$$\eta_1 = \sqrt{v_A/\tilde{v}_1}\cos\theta, \ \eta_2 = \sqrt{v_A/\tilde{v}_2}\sin\theta, \quad (A12)$$
$$\lambda_1 = -\sqrt{v_a/\tilde{v}_1}\sin\theta, \ \lambda_2 = \sqrt{v_a/\tilde{v}_2}\cos\theta. \quad (A13)$$

[1] B. Paredes, A. Widera, V. Murg, O. Mandel, S. Foelling, I. Cirac, G. V. Shlyapnikov, T. W. Hänsch, and I. Bloch, Nature **429**, 277 (2004).

[2] T. Kinoshita, T. Wenger, and D. S. Weiss, Science 305, 1125 (2004).

[3] T. Stöferle, H. Moritz, C. Schori, M. Köhl, and T. Esslinger, Phys. Rev. Lett. **92**, 130403 (2004).

[4] C. D. Fertig *et al*, cond-mat/0410491.

[5] H. Moritz, T. Stöferle, K. Günter, M. Köhl, and T. Esslinger, Phys. Rev. Lett. **94**, 210401 (2005).

[6] A. Recati, P. O. Fedichev, W. Zwerger, and P. Zoller, Phys. Rev. Lett. **90**, 020401 (2003); J.N. Fuchs, A. Recati, and W. Zwerger, Phys. Rev. Lett. **93**, 090408 (2004).

[7] M. A. Cazalilla, A.F. Ho, and T. Giamarchi, Phys. Rev. Lett. **95**, 226402 (2005).

[8] M. A. Cazalilla and A. F. Ho, Phys. Rev. Lett. **91**, 150403 (2003).

[9] L. Mathey, D.-W. Wang, W. Hofstetter, M. D. Lukin, and E. Demler, Phys. Rev. Lett. **93**, 120404 (2004).

[10] L. Mathey, and D.-W. Wang, Phys. Rev. A 75, 013612 (2007).

[11] P. Sengupta and L. P. Pryadko, cond-mat/0512241.

[12] A. Isacsson and S. M. Girvin, Phys. Rev. A 72, 053604 (2005); A. Isacsson, M.-C. Cha, K. Sengupta, and S. M. Girvin, Phys. Rev. B 72, 184507 (2005).

[13] A.B. Kuklov, and B.V. Svistunov, Phys. Rev. Lett. **90**, 100401 (2003); A.B. Kuklov, Nikolay Prokofev, and B.V. Svistunov, Phys. Rev. Lett. **92**, 030403 (2004).

[14] M. Greiner, O. Mandel, T. Esslinger, T. W. Hänsch, and I. Bloch, Nature (London) **415**, 39 (2002).

[15] Due to the confining trap the transition is, while visible, 'blurred' into a gradual cross-over, due to finite size effects, and, more importantly, due to the coexistence of several phases in the trap. This can also be expected for the phase transitions predicted in this paper.

[16] G.B. Partridge, W. Li, R. I. Kamar, Y. Liao, and R. G. Hulet, Science **311**, 503-505 (2006); M. Zwierlein, A. Schirotzek, C. H. Schunck, and W. Ketterle, Science **311** (5760), 492–496 (2006).

[17] M.A. Cazalilla and A.F. Ho, Phys. Rev. Lett. **91**, 150403 (2003).

[18] F. D. M. Haldane, Phys. Rev. Lett. **47**, 1840 (1981); M.A. Cazalilla, J. Phys. B: AMOP 37, S1–S47 (2004).

[19] J. Voit, Rep. Prog. Phys., **58**, 977 (1995).

[20] T. Giamarchi, *Quantum Physics in one dimension*, Clarendon Press (Oxford, UK, 2004).

[21] J. B. Kogut, Rev. Mod. Phys., **51**, 659 (1979); A.O. Gogolin, A.A. Nerseyan and A.M. Tsvelik, *Bosonization and Strongly Correlated Systems* (Cambridge University Press, 1998).

[22] M. Greiner, C. A. Regal, J. T. Stewart, and D. S. Jin, Phys. Rev. Lett. **94**, 110401 (2005); S. Foelling, F. Gerbier, A. Widera, O. Mandel, T. Gericke, and I. Bloch, Nature **434**, 481 (2005); E. Altman, E. Demler, and M. D. Lukin, Phys. Rev. A **70**, 013603 (2004); L. Mathey, E. Altman, and A.Vishwanath, cond-mat/0507108; L. Mathey, E. Altman, and A.Vishwanath, in preparation.

[23] C. Chin, M. Bartenstein, A. Altmeyer, S. Riedl, S. Jochim, J. Hecker Denschlag, and R. Grimm, Science **305**, 1128 (2004).